Drought Legacies Mediated by Trait Tradeoffs in Soil Microbiomes

Bin Wang [1], Steven D. Allison [1,2]

[1] Department of Ecology and Evolutionary Biology, University of California, Irvine, CA

[2] Department of Earth System Science, University of California, Irvine, CA

Abstract: Soil microbiomes play a key role in driving biogeochemical cycles of the Earth system. As drought frequency and intensity increase due to climate change, soil microbes and the processes they control will be impacted. Even after a drought ends, microbiomes and other systems take time to recover and may display a "memory" of previous climate conditions. Still, the mechanisms involved in these legacy effects remain unclear, making it difficult to predict climate and biogeochemical rates in the future. Here, we used a trait-based microbiome model to analyze mechanisms underlying drought legacy effects on litter decomposition. We represented cellular tradeoffs between osmolytes required for drought tolerance and investment in enzymes involved in litter decomposition. Simulations were run under varying levels of drought severity and dispersal. When dispersal was restricted, we found persistent drought legacies following severe drought and transient legacies following moderate drought. With dispersal, there were no legacy effects on litter decomposition. Greater movement along the tradeoff between enzyme investment and osmolyte production resulted in stronger legacy effects. We organized these legacy outcomes according to the YAS framework defined by tradeoffs between Y (Yield), A (Acquisition), and S (Stress tolerance), three primary life history strategies of microorganisms. Factors that change the trajectory of a community in YAS space may alter the legacy outcome following drought. This trait-based mechanistic insight into drought legacies offers promise for more accurately predicting soil microbiome resilience and functioning. Our study illustrates an emerging approach for representing trait tradeoffs in microbiome and vegetation that dictate ecosystem responses to drought and other environmental perturbations.

1 Introduction

Drought of increasing severity and frequency both regionally and worldwide is an important environmental change affecting the Earth system (e.g., **Borsa et al. 2014; Berdugo et al. 2020**). The soil microbiome is a key driver of element cycling (e.g., **Falkowski et al. 2008**), so microbial responses are integral for evaluating drought impacts on ecosystem biogeochemistry. Still, these responses are omitted or implicitly treated in global assessments of drought-biosphere interactions (e.g., **Green et al. 2019**).

Over a-half century of research has uncovered a myriad of physico-chemical, physiological, and ecological mechanisms underlying microbial functional responses to drought disturbance in soil environments (e.g., **Birch 1958; Schimel 2007; Manzoni et al. 2012**). However, multiple studies have suggested that drought may have lasting effects on the soil microbiome and its functioning, even after drought conditions have ended (e.g., **Evans and Wallenstein 2012**; **Meisner et al. 2015**; **Hawkes et al. 2017; Martiny et al. 2017; Hinojosa et al. 2019**). This phenomenon, here termed drought legacy, has also been observed in forests and other biomes (e.g., **Cuddington 2011; Anderegg et al. 2015; Conradi et al. 2020**). Still, the mechanistic basis for microbial drought legacies remains unclear. Such a lack of mechanistic insights hinders the ability to predict drought impacts on ecosystem processes.

Legacies likely originate from microbiome changes that persist after a drought disturbance. Microbiomes are complex adaptive systems, with their functioning emerging from both individual variation and within-community interactions. Past lab- and field-based studies explained soil microbial drought legacies by depicting compositional differences in terms of microbial functional groups with different life-history strategies. Notably, **Hawkes and Keitt (2015)** proposed a mechanism of community shift in relative abundance of moisture generalists vs. specialists, where

generalists are functionally more stable than specialists with variations in moisture. This idea was proposed to explain a lack of change in moisture response across sites in Texas, USA, because of observed dominance by generalist taxa resulting from high variability in historical rainfall (**Hawkes et al. 2017; Waring and Hawkes 2018**). Similarly, **Evans and Wallenstein** (**2014**) argued soils with relatively stable moisture history had more moisture-sensitive taxa and hence larger changes in biomass and composition following drought (**Evans and Wallenstein 2012**).

Conceptual frameworks of microbial legacies based on functional groups can help simplify complex microbiomes but may obscure important physiological and ecological details. For instance, microbial cells can re-direct resource allocation from exoenzyme production to osmolytes that confer desiccation resistance (e.g., **Schimel 2007**), an intra-cellular metabolic strategy that displays large inter-cellular variability (e.g., **Manzoni et al. 2012**). Without representing these physiological processes, models may have difficulty predicting microbial community responses to drought disturbance and the consequences for functioning. Addressing this challenge could help reconcile studies that report drought legacies of varying magnitudes with differing time frames, including those that observed no legacy (e.g., **Rousk et al. 2013; Fuchslueger et al. 2016**). A similar lack of mechanistic understanding also applies to warming-induced legacies in microbiome functioning (e.g., **Karhu et al. 2014**). Linking individual-level physiological variation to community-level shifts could help fill this gap in knowledge of microbial functioning with environmental change.

Trait-based approaches for dealing with ecological complexity can bridge the gap between community dynamics and physiological variation that may underpin drought legacies in microbiomes. Such approaches have been established previously in plant communities (e.g., **McGill et al. 2006**), and more recently, **Malik et al. (2020)** proposed a trait-based framework—

Y-A-S (Yield-Acquisition-Stress)—that emphasizes tradeoffs among three primary life history strategies of microorganisms. On the empirical side, a manipulative experiment in a grassland ecosystem in Southern California attributed a drought legacy in litter decomposition to changes in bacterial composition and associated carbohydrate degradation traits (**Martiny et al. 2017**). This study illustrates the potential to establish trait-based linkages between microbial physiology and community shifts underlying legacies.

Based on the Y-A-S framework, drought disturbance should cause cellular physiology and microbial composition to shift toward drought tolerance at the expense of other traits, such as investment in exoenzymes. Persistence of this functional shift could result in a drought legacy that affects organic matter decomposition. With this reasoning, factors that shift microbiomes along the tradeoff between enzyme investment and stress tolerance could alter the magnitude and duration of drought legacies. For instance, the intensity of drought, which directly modulates intracellular metabolic allocation to enzymes versus osmolytes (e.g., **Csonka 1989; Schimel 2007**), may determine movement along the tradeoff and hence affect the legacy magnitude. In addition, microbial dispersal (e.g., **Fukami 2015; Vila et al. 2019**) may alter drought legacies through effects on community composition and dynamics that regulate drought-tolerance tradeoffs (**Hawkes et al. 2017**). Therefore, we hypothesize that trait-based tradeoffs between drought tolerance and enzyme investment govern drought legacies in soil microbiomes.

Theory-driven, trait-based models are well positioned to complement lab- and field-based studies and test the mechanisms underpinning soil microbiome drought legacies. Individual-based models in particular offer the ability to bridge scales from individual cells through communities to ecosystems by explicitly simulating intra-cellular metabolic processes, ecological dynamics of microbial communities, and emergent functioning (**Allison 2012**). Such an approach can overcome

some of the limitations of aggregated models that treat microbes as a single biomass pool or a few discrete functional groups [see a review by **Wieder et al. (2015**)]. In addition, trait- and individual-based models are appropriate for testing the null hypothesis that representing legacies would have little impact on biogeochemical model predictions (**Rousk et al. 2013**).

The goal of our study was to analyze the trait-based, tradeoff-mediated mechanisms underpinning drought legacies in soil microbiomes. Our approach applied a modelling framework for soil microbial systems—DEMENTpy—that represents tradeoffs among resource acquisition and drought tolerance at the physiological level along with emergent processes at the community level. This individual- and trait-based model represents physiological mechanisms in a spatially-explicit context. Specifically, we asked the following questions: 1) How does the magnitude of drought legacy vary with drought intensity for the process of litter decomposition? 2) How does microbial dispersal affect the duration and magnitude of drought legacy? 3) What are the underlying changes in enzyme investment and drought tolerance traits? And 4) how do these changes align with the mechanisms proposed in the Y-A-S framework? We tackled these questions by applying DEMENTpy to a grassland ecosystem in Southern California. Our study exemplifies how trait-based investigations into microbiome legacies can improve mechanistic understanding of element cycling in response to climate change.

2 Methods

2.1 Model description

DEMENTpy (DEcomposition Model of ENzymatic Traits in Python; GitHub Repository: https://github.com/bioatmosphere/DEMENTpy) is a spatially-explicit, trait- and individual-based model. Starting from continuous physiological traits, DEMENTpy bridges across soil microbiome

scales from individual cells through communities and systems (see **Supporting Fig. 1** for model structure). Its mechanistic modelling framework is built upon its predecessor DEMENT (**Allison 2012; Allison and Goulden 2017; Wang and Allison 2019**). DEMENTpy initiates a microbial community composed of a large number of hypothetical taxa by randomly drawing values from uniform distributions of microbial traits and assigning them to different taxa (see a list of traits in **Supporting Fig. 1B** and more details in **Supporting Text**). Community dynamics are simulated by explicitly modelling demographic processes of cell metabolism and growth, mortality, and reproduction for each taxon population at a daily time step. Microbial taxa secrete exoenzymes (constitutive and inducible) that degrade different organic compounds at rates that depend on temperature and moisture. To address questions related to drought response, the current version of DEMENTpy represents explicit osmolyte production (constitutive and inducible). Drought tolerance of each taxon is determined by normalizing the inducible osmolyte rate of production to a value from 0 to 1. This formulation establishes a mechanistic connection between osmolyte production and drought tolerance (**Schimel 2007**) in contrast to the previous model version which instead directly introduced a drought tolerance parameter and imposed a penalty on carbon use efficiency accordingly (**Allison and Goulden 2017**).

DEMENTpy tracks intra-cellular metabolism of assimilated monomer carbon derived from exoenzymatic degradation of substrates (**Supporting Fig. 1C**; see **Supporting Text** for substrate degradation and other demographic processes). After growth respiration, assimilated carbon is directed to enzyme production, osmolyte production, and associated maintenance respiration, which are treated as simultaneous processes without prescribing an order. The carbon remaining after constitutive and inducible metabolite production accumulates toward biomass (denoted as yield). We assume that constitutive osmolyte production varies across taxa but independent of

water potential, reflecting microbial allocation to maintain water potential balance across the cell wall (e.g., **Csonka 1989; Potts 1994**). By contrast, inducible production of osmolytes occurs when water potential falls below a threshold. Mortality of microbial cells is simulated both deterministically by accounting for mass balance and stochastically based on death probability dependent on drought tolerance and water potential. More details on model structure, processes, formulae, and parameters are included in the **Supporting Information.**

2.2 Modelling experiments

We applied DEMENTpy to a grassland ecosystem at Loma Ridge, Southern California (**Allison et al. 2013**) and parameterized the model with 100 different hypothetical bacterial taxa on a 100 by 100 spatial grid with decomposing grass litter containing ten different substrates (see parameter values in **Supporting Table 1** and substrates in **Supporting Table 2**). DEMENTpy was forced with daily weather data from the year 2011, which is designated as the ambient scenario (**Supporting Fig. 2A)**. In addition to this ambient scenario, we conducted simulations to examine drought disturbance response and recovery in three phases (**Supporting Fig. 2**). Two drought scenarios, moderate and severe, were generated by reducing the water potential during the dry season by a factor of four and ten, respectively. After a community establishment phase and a successive drought period, ambient conditions were re-imposed to test for legacy effects on microbial communities and substrate decomposition. Simulations in "default" mode did not allow for microbial dispersal; once taxa disappeared from a default simulation, they could not return. We also ran simulations in "dispersal" mode to test how dispersal affects drought response and legacy effects. In contrast to the default mode, dispersal mode allows extinct taxa to recolonize at the start of each model year. This mode accounts for the possibility that bacterial populations survive in local refugia or nearby wetter areas and then disperse on to fresh litter.

2.3 Simulation protocol

After establishing an initial microbial community from a randomly constructed microbial pool on the spatial grid with homogeneously distributed substrates, each simulation was run for 10 years at a daily time step (spin-up: 3 years; drought disturbance: 3 years; recovery: 4 years) (**Supporting Fig. 2**). Substrates, monomers, and enzymes were reinitialized uniformly on the spatial grid at the start of each new year to have the same concentrations as the first year. At the start of each year, the microbial community on the spatial grid was randomly reinitialized with the same total microbial biomass. Two reinitialization methods were applied to differentiate between the default and dispersal modes: for the default mode, microbial community composition was determined according to the biomass frequency of each taxon on the last day of the previous year (**Supporting Fig. 2C**); in dispersal mode, the taxon frequencies were based on the cumulative biomass of each taxon across the entire previous year (**Supporting Fig. 2D**). Simulations were repeated 40 times for each scenario under the two modes (default and dispersal) with 40 different random number generation seeds ($5 \times 40 = 200$ runs in total). This sample size was determined by a convergence analysis of DEMENTpy's stochastic nature (**Supporting Fig. 3**).

2.4 Data analysis

Unless indicated otherwise, all analyses were conducted on the ensemble of 40 runs for each of the five scenarios. Datasets extracted from these simulations included: taxon traits (enzyme investment and drought tolerance); a time-series of taxon-specific allocation to enzymes (inducible plus constitutive); osmolytes (inducible plus constitutive); yield and biomass in carbon; and a time-series of compound-specific and total substrate concentrations. Taxon-specific allocations to enzymes, osmolytes, and yield were aggregated to derive the corresponding community-level allocation. Community-level traits of enzyme investment and drought tolerance were calculated

206 from biomass-weighted taxonomic traits (see the **Supporting Text** for calculation method).
207 Because the system stabilized within 3 years (**Supporting Fig. 2**), results up to year 9 (3rd year of
208 recovery from drought disturbance) are presented. In addition, 95% confidence intervals are shown
209 for most variables except for microbial community composition and community carbon allocation,
210 for which only one out of the 40 simulations are shown.
211

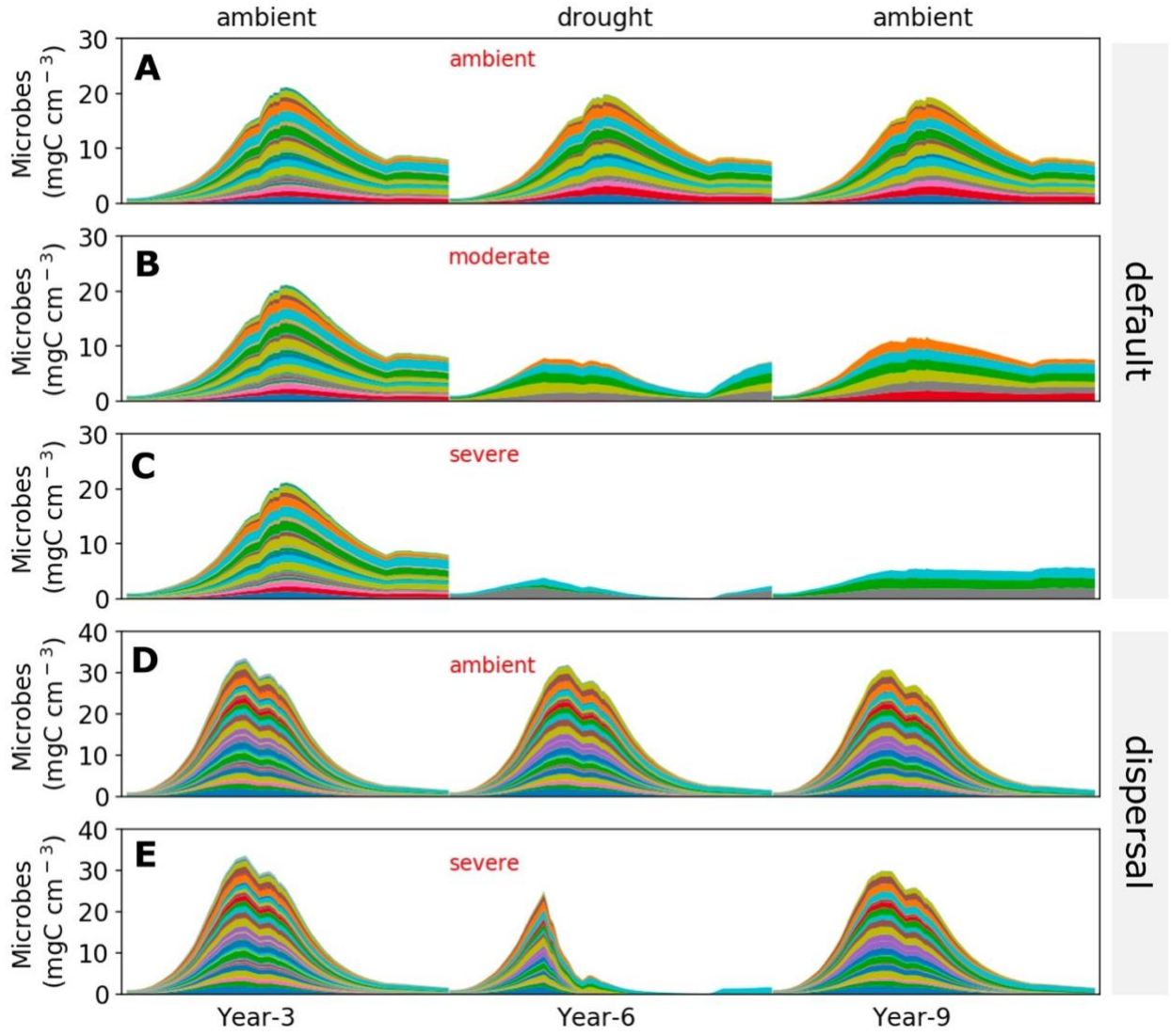

212

213 **Fig. 1. Microbial community dynamics in ambient and drought simulations with and without**
214 **dispersal.** (**A-C**) Dynamics without dispersal under ambient, moderate, and severe drought

scenarios, respectively. (**D, E**) Dynamics with dispersal under ambient and severe drought scenarios, respectively. Colored bands represent biomass of hypothetical taxa (mg C cm^{-3}) averaged over the 100×100 spatial grid. Data shown are only for years 3, 6 (the 3rd year under drought), and 9 (the 3rd year after drought). See **Supporting Fig. 2** for the full 10-year dynamics under the ambient scenario of both default and dispersal mode.

3 Results

3.1 Microbial community dynamics under the ambient drought scenario

The system became relatively stable after 2 years, with seasonal dynamics in the microbial community repeating across years (**Supporting Fig. 2**). Seasonal dynamics of community composition and biomass reflected a joint control by climate and substrates. Starting in the wet season that was replete with substrates, the microbial community established and grew in biomass. As substrates were degraded and depleted, microbial cells began to starve and die. Declining water potentials after the start of the dry season induced more death. Together, these two processes resulted in declining microbial biomass from a peak around 20 mg C cm^{-3} (**Fig. 1A)** and drove the composition toward taxa with higher drought tolerance and lower enzyme investment (**Supporting Fig. 4A**). Hence community level enzyme investment decreased (**Fig. 2A**), and drought tolerance increased across the dry season (**Fig. 2B**). Similar seasonal and inter-annual dynamics were observed for the community with dispersal but with much higher biomass (peaking around 30 mg C cm^{-3}) and taxonomic diversity (**Fig. 1D; Supporting Fig. 4B; Fig. 2C, D**).

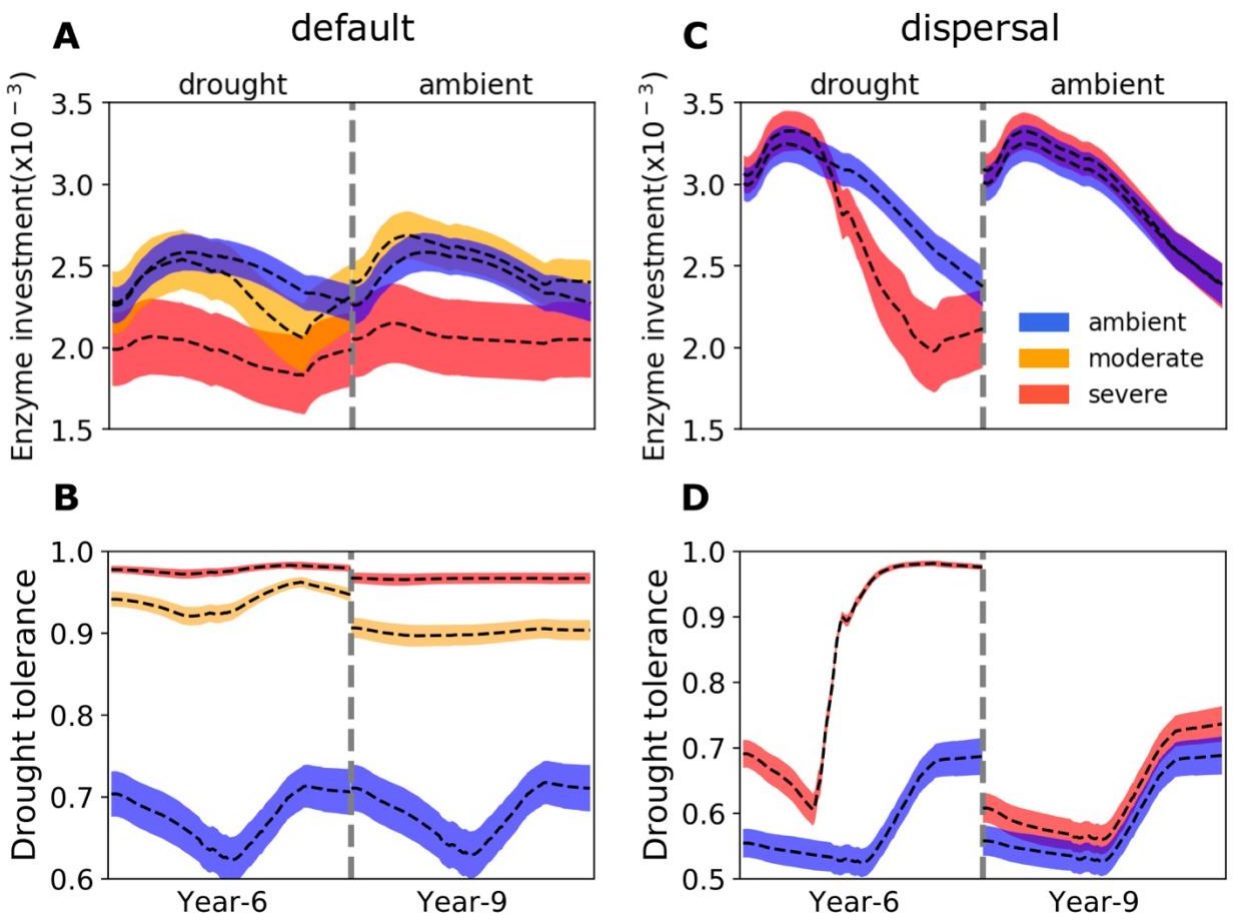

Fig. 2 Seasonal dynamics of community-level enzyme investment and drought tolerance of microbial communities under different drought scenarios. (**A, B**) Enzyme investment and drought tolerance during year 6 (3rd year under drought) and year 9 (3rd year after drought) under three drought scenarios (ambient, moderate, and severe) without dispersal, respectively. (**C, D**) The same for communities with dispersal under two drought scenarios (ambient and severe). Dashed lines and color bands are means and 95% confidence intervals (n=40).

3.2 Responses to drought disturbance of varying severity

Total microbial biomass declined significantly under drought, with the greatest declines of nearly 50% under the severe scenario, resulting in a peak biomass less than 10 mg C cm^{-3} (**Fig.**

1B, C). Severe drought also more drastically altered microbial community composition compared to moderate drought. Community taxonomic richness and functional capacity shifted dramatically after 2 years of drought perturbation. Compared to the ambient scenario, drought tolerance increased significantly across seasons from 0.62 up to 0.92 under the moderate scenario and up to 0.97 under the severe scenario (**Fig. 2A,B**). However, the community-averaged enzyme investment only declined significantly in the severe scenario across the dry season and did not change substantially in the moderate scenario except late in the dry season (**Fig. 2A,B**). These trait changes reflected differences in community-level carbon allocation between enzymes and osmolytes and thus yield (**Fig. 3A; Supporting Fig. 5A**). Under the moderate drought scenario, the percentage of assimilated carbon allocated to osmolytes ranged between 65% and 85%, compared to the ambient range of 50% to 70%, whereas enzyme allocation was consistently lower (10% on average) compared to the ambient scenario (20% on average). However, the resulting yield was similar, ranging between 0 and 30%, although some days in the ambient scenario were higher (reaching at most 40%) early in the drought season. Under the severe scenario, the allocation to osmolytes was even higher and allocation to enzymes even lower, and the community yield approached zero more often. These differences in community resource allocation resulted in reduced degradation of substrates over the grid, with the two drought scenarios showing different rates of decomposition (average of 57.39 and 85.65%, respectively; **Fig. 4A, B**).

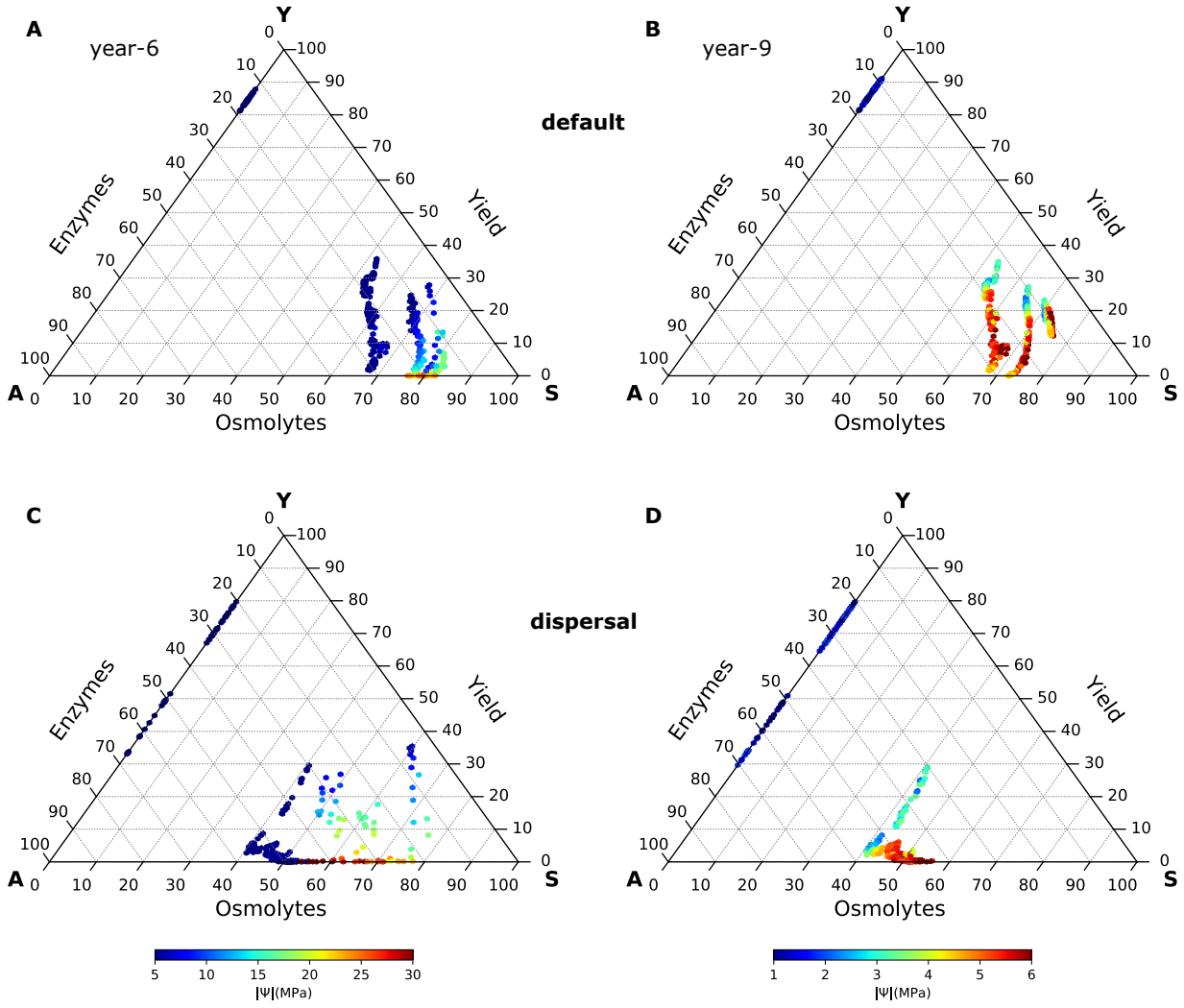

Fig. 3 Ternary plots of community-level allocation of assimilated carbon among enzymes, osmolytes, and growth yield over time under different dispersal scenarios. (A, B) Enzyme-Osmolyte-Yield tradeoff of communities during year 6 (3rd year under drought) and year 9 (3rd year after drought), respectively, of the default mode (without dispersal). (**C, D**) The same for the dispersal mode. Yield, enzymes, and osmolytes correspond to Y (Yield), A (resource Acquisition), and S (Stress) strategies labeled respectively at the triangle vertices (**Malik et al. 2020**). See **Supporting Fig. 5** for a version with points differentiated by drought scenario instead of water potential.

After ambient conditions were re-imposed for 2 years (i.e., by year 9), new stable microbial communities assembled (**Fig. 1B, C** and **Supporting Fig. 2C**). Compared to the ambient scenario, communities that re-assembled following drought had different levels of drought tolerance and enzyme investment. Compared to the ambient scenario, drought tolerance remained significantly higher under both the moderate drought (0.90) and severe drought (0.96) scenarios, even after drought disturbance ended (**Fig. 2A**). In contrast, enzyme investment under the moderate scenario became similar to the ambient community, with only the community re-assembling after severe drought remaining significantly different (**Fig. 2B**). During the dry season by year 9, only the severe-drought community showed a clearly lower allocation to enzymes compared to the ambient community season (**Fig. 3B; Supporting Fig. 5B**). This resilience of enzyme investment in the moderate-drought community meant that decomposition rates converged on ambient levels by year 9 (**Fig. 4A**). In contrast, substrate mass loss remained lower by 47.72% on average (**Fig. 4A**) in year 9 of the severe drought scenario, although the magnitude of decline was dampened compared to the antecedent drought period. Prior to year 9, the reductions in mass loss associated with transient microbial communities (year 7) were significant for both drought scenarios (average declines of 18.00 and 55.52%, respectively).

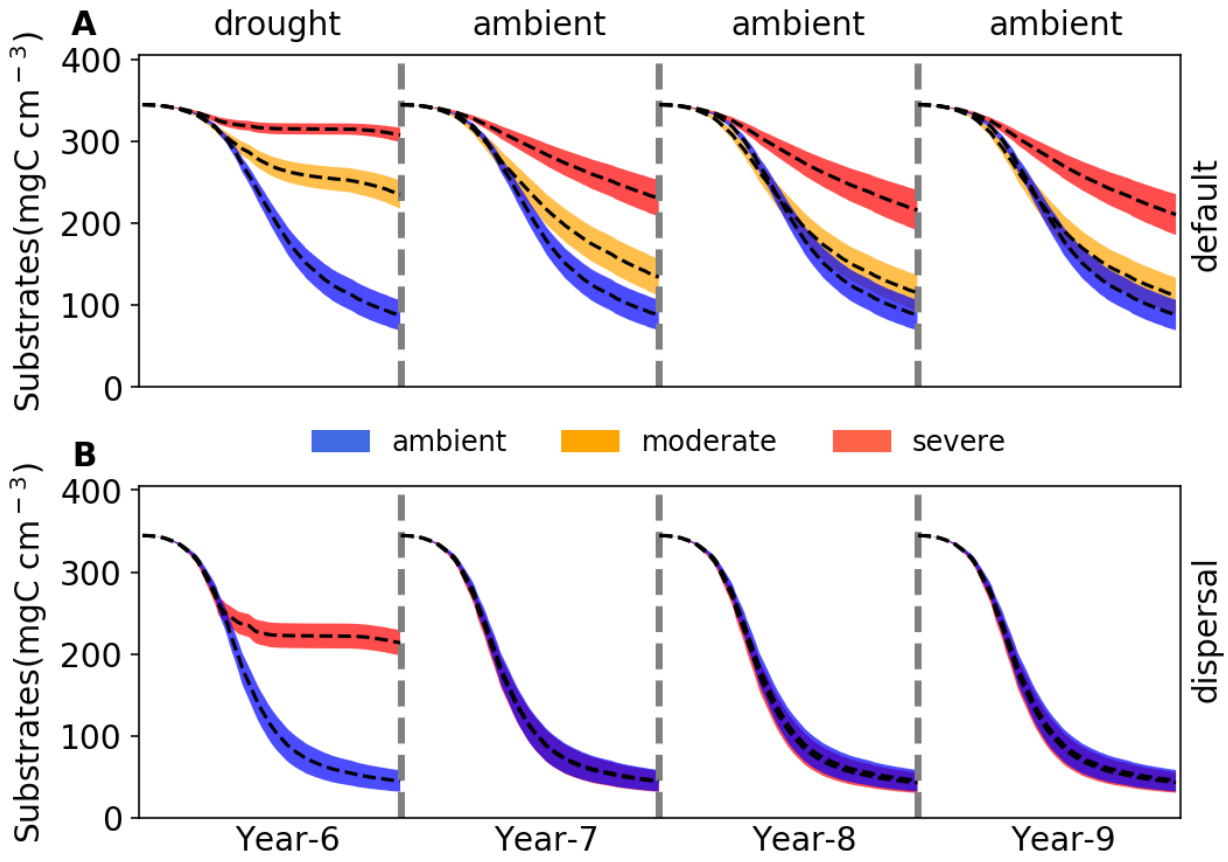

Fig. 4 Changes in substrate concentrations as litter decomposes during and after drought perturbation. (**A**) Total substrates on the spatial grid during years 6 (last year of drought) to 9 under three different scenarios (ambient, moderate, and severe drought) without dispersal. (**B**) The same for simulations with dispersal under ambient and severe drought scenarios. Dashed lines and colored bands are means and 95% confidence intervals (n = 40), respectively. See **Supporting Fig. 6** for an example illustration of the underlying substrate-specific changes.

3.3 Responses to severe drought disturbance with dispersal

With dispersal of taxa from the same microbial pool at the start of each year, the direct responses to severe drought were similar to the default mode, though with differing magnitudes and seasonal patterns. With dispersal during drought disturbance, the microbial community

showed both lower total biomass and reduced taxonomic richness, particularly during the dry season, though the values were higher than in the default mode (**Fig. 1E**). Community-average enzyme investment and drought tolerance differed from the ambient scenario but with a different seasonal pattern compared to the default mode. With the onset of the dry season, enzyme investment declined sharply from a peak of 0.0033 down to 0.0020, and drought tolerance increased sharply from 0.60 to 0.97, with differences from the ambient scenario increasing over time (**Fig. 2C,D**). These changes reflected the community allocating more assimilated carbon to produce osmolytes and less to enzymes, which resulted in zero yield when drought was most severe during the dry season (**Fig. 3C; Supporting Fig. 5C**). All of these changes resulted in significantly lower substrate decomposition (**Fig. 4A**; an average decline of 56.29%).

When ambient conditions were re-imposed, recovery from drought was rapid compared to the default mode. Two years after drought ended, the communities became similar in the drought and ambient scenarios (**Fig. 1E**), a stark contrast to the default mode (**Fig. 1C**). This compositional similarity coincided with similar community enzyme investment (**Fig. 2C**) and drought tolerance (**Fig. 2D**), which resulted in the same community-level allocation of assimilated carbon among enzymes (30 - 60%), osmolytes (40 - 60%), and thus yield (0 - 30%; **Fig. 3D; Supporting Fig. 5D**). These communities ultimately had almost exactly the same composition and substrate decomposition rates (**Fig. 4B**). In fact, in contrast to the default mode, the transient community did not even show significant differences in the 1st year following drought (year 7; **Fig. 4B**). Based on this clear lack of legacy effects following severe drought, we did not find it relevant to run simulations of the moderate scenario with dispersal.

4 Discussion

By applying trait-based modelling in a mechanistically-explicit fashion, we tested the relationships between drought legacy and drought severity and dispersal in simulated litter microbiomes. Drought legacy effects on litter decomposition ranged from persistent through transient to no legacy at all and depended on drought severity and microbial dispersal (**Fig. 4**). This variation in legacy magnitude and duration showed a clear mechanistic basis—tradeoffs between enzyme production and drought tolerance, in line with the Y-A-S strategy framework. These results are relevant for understanding the resilience of microbial systems—weaker legacies correspond to higher resilience of soil microbiome functioning in response to historical drought. Our analysis of legacy mechanisms underlying microbial system resilience will help more accurately quantify carbon cycle feedbacks to drought in the Earth system.

Transient legacy under moderate drought

The severity of drought disturbance influences legacy magnitude and duration by determining the extent to which a microbial community can adapt (**Fig. 4A**). Our drought disturbance lasted long enough for communities to reach a stable state. However, our simulations focused on testing underlying mechanisms and only represent a subset of actual drought disturbances in terms of frequency, intensity, and duration. At the drought intensities we analyzed, legacies ranged from transient to persistent. Weaker disturbances might result in no legacy at all.

Drought disturbance of lower severity had a negative effect on decomposition conferred by the transient community, but eventually the legacy effect disappeared (**Fig. 4A**), a pattern that we dub “transient legacy”. This transient legacy pattern matches results from a reciprocal transplant manipulation of microbial communities within a rainfall manipulation experiment at our

Loma Ridge field site where we observed full recovery in terms of litter decomposition after one year (**Martiny et al. 2017**). It is noteworthy that our model-predicted transient legacy arose from a community with the same functioning but different composition and biomass. However, with a total biomass difference varying from 50% to essentially no difference (**Fig. 1B**), the link between total biomass and functioning is likely not a major driver of the legacy pattern, consistent with findings from our field experiment (**Martiny et al. 2017**) and another reciprocal transplant study across a climate gradient in Southern California (**Glassman et al. 2018)**. Rather, the transience of the legacy mainly resulted from convergence in community enzyme investment despite lingering differences in community composition and drought tolerance (**Fig. 2A,B**). Such a compositional but not functional change in an ecosystem after disturbance—which has been observed before (e.g., **Fukami 2015; Ives and Carpenter 2007**)—supports the notion of functional similarity in the soil microbiome (**Allison and Martiny 2008**). It is this transient legacy that allows for resilience of microbial and other systems following moderate perturbation. Particularly in microbial systems, functional redundancy may contribute to this resilience (e.g., **Louca et al. 2018**).

Persistent legacy under severe drought

A strong drought disturbance can push a community to reach an even higher drought tolerance by sacrificing more investment in enzyme production (including a loss of relatively more drought-intolerant taxa), thereby forming a community not only compositionally but also functionally different (**Fig. 2A,B**). These conditions can lead to a persistent legacy (**Fig. 4B**). A similar long-term legacy in soil heterotrophic respiration has also been observed in microcosm and field transplant experiments (**Hawkes et al. 2017)**. This persistent legacy is consistent with the idea of alternative stable states with different functioning in ecological systems (**Scheffer et al.**

2001). Disturbance-driven alternative stable states have been reported across an array of systems; e.g., in gut microbiota experiencing transient osmotic perturbation (**Tropini et al. 2018**) and in tropical (e.g., **Staver et al. 2011**) and boreal forests (**Herzschuh 2020**), as well as in small pond systems (**Chase 2003**). Conceptually, a persistent legacy means the loss of system resilience with severe disturbance (**Scheffer et al. 2001**).

Disappearance of legacy under severe drought with dispersal

Importantly, dispersal can exclude legacies in organic matter decomposition (**Fig. 4B**). By re-introducing taxa from the previous year's microbial pool, we found that even with severe drought, dispersal can rescue taxa from extinction and completely mitigate the effect of environmental selection on the microbial community (**Fig. 1E**). By re-introducing drought tolerance and enzyme investment traits (**Fig. 2C,D; Fig. 3D**), dispersal can overwhelm the drought legacy in organic matter decomposition (**Fig. 4B**). This result suggests that dispersal can increase microbial systems' resilience to drought disturbance (**Allison and Martiny 2008**) in stark contrast to the persistent legacy induced by severe drought disturbance without dispersal (**Fig. 4B**). We note that there are many dispersal factors that influence community dynamics but were not represented in our model. For instance, dispersal timing (e.g., priority effects) and size both matter for community response to perturbation (e.g., **Fukami 2015; Vila et al. 2019**). Furthermore, even an unsuccessful invasion by a single species that interacts only briefly with the resident community can induce an alternative stable state with distinct functioning (**Amor et al. 2020**). Variation in dispersal processes could therefore drive compositional and functional changes to varying extents (e.g., **Fukami 2015**), resulting in varying magnitudes of decomposition legacy. For example, in a field transplant experiment with passive dispersal, **Hawkes et al. (2017)** did not find apparent

mitigation of historical rainfall legacy in soil respiration. Given this result, we recognize that our exploration of dispersal mechanisms and intensities is incomplete; our study was mainly aimed at revealing underlying mechanisms and not meant to be exhaustive.

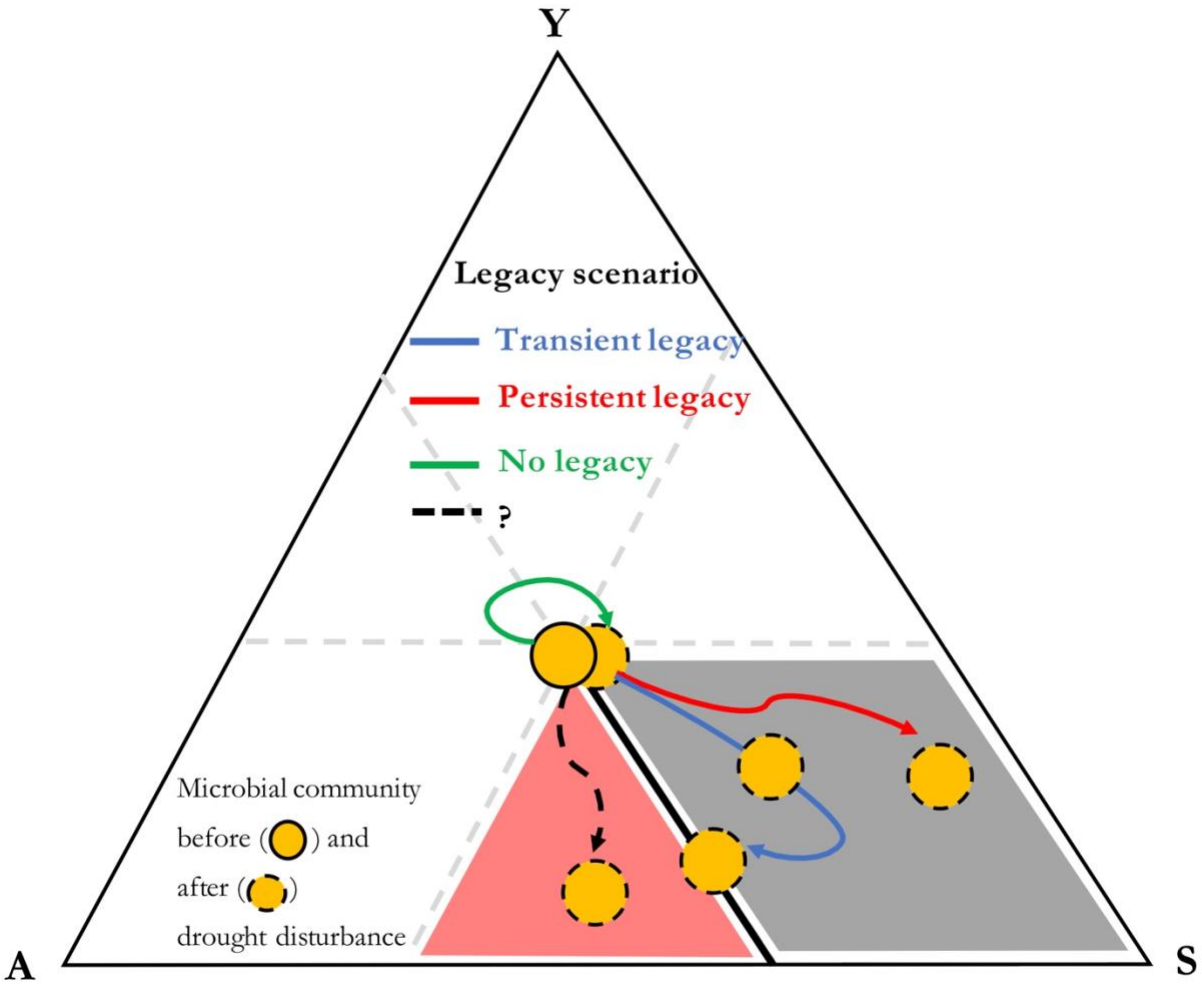

Fig. 5 Overlay of drought legacy scenarios in YAS-constrained space. Drought legacy is contingent on the trajectory of a microbial community in the YAS space after drought disturbance. There will be no legacy if a community does not move at all (green trajectory) or if it moves along the thick black line. If an altered community remains in the grey region, a persistent legacy will occur. However, if the community eventually leaves the grey region and returns to the thick black line, a transient legacy can occur. We also propose that a community could move into the red

region with both increased drought tolerance and enzyme investment (but at the expense of growth yield). Note: the positioning of the starting community in the center of the space (filled yellow circle) is for illustration purposes only; real communities may start anywhere in the YAS space.

A mechanistic conceptual framework

We propose to organize legacy scenarios based on the YAS framework, as illustrated in **Fig. 5**. Drought legacies are ultimately determined by the trajectory of a community in a conceptual space defined by enzyme investment, drought tolerance, and yield. Factors that affect cellular metabolic and community-level tradeoffs between enzyme and osmolyte production may influence the magnitude and/or duration of a drought legacy. For instance, when drought selects for a community with higher drought tolerance but ultimately similar enzyme investment (e.g., moderate drought scenario; **Fig. 4A**), a transient legacy occurs. However, when more severe drought selects for higher drought tolerance at the expense of enzyme investment (**Fig. 4A**), a persistent legacy with impaired substrate decomposition can occur. In contrast, when the community does not shift in strategy space (e.g., with dispersal present; **Fig. 4B**), even transient legacies may not occur.

Tradeoffs in microbiomes and the biosphere more generally are often complex (e.g., **Berezovsky & Shakhnovich 2005; Ferenci 2016**). Some tradeoffs may be context-specific, and even positive relationships between costly traits may be observed under certain conditions (**Moreno-Gámez et al. 2020; Tikhonov et al. 2020**). These principles may apply to the relationship between enzyme investment and drought tolerance which may depend on drought intensity, dispersal, metabolic plasticity, and evolution history. For instance, a fourth legacy scenario may exist with both increased osmolyte and enzyme investment that trade off against

lower yield (the red region in **Fig. 5**). Going forward, our study could be extended by broadening the range of drought and dispersal scenarios and modifying the tradeoff assumptions in DEMENTpy to gain a more complete picture of the mechanisms underlying drought legacies.

Implications

Our study revealed a tradeoff-mediated explanation for community-level trait changes that lead to drought legacies in soil microbiomes. This mechanistic insight has consequences for ecosystem responses to drought and other environmental changes. A more accurate quantification of the magnitude and duration of drought legacies should enable better predictions of litter and soil organic matter decomposition. Legacies of impaired decomposition, even when transient, may enhance carbon sequestration in soil systems, but may also allow fuels to accumulate for the next fire season, thereby increasing fire risk (e.g., **Pellegrini et al. 2018**). Additionally, impaired decomposition can inhibit nutrient turnover and availability, thereby influencing plant productivity and interactions with microbes (e.g., **Kaisermann et al. 2017**). These and other cascading changes arising from microbiome legacies could initiate more complex ecosystem feedbacks. Evaluating these implications requires a holistic approach that integrates microbial and vegetation processes across ecosystem to Earth system scales. Such an approach is crucial for predicting biogeochemical rates in the context of projected global climate change that may induce legacy effects. Trait-based models of both microbial and vegetation dynamics are proving essential in achieving this predictive understanding.

References

Allison, S. D. (2012). A trait-based approach for modelling microbial litter decomposition. Ecology letters, 15, 1058-1070.

Allison, S. D., & Goulden, M. L. (2017). Consequences of drought tolerance traits for microbial decomposition in the DEMENT model. Soil Biology and Biochemistry, 107, 104-113.

Allison, S. D., Lu, Y., Weihe, C., Goulden, M. L., Martiny, A. C., Treseder, K. K., & Martiny, J. B. (2013). Microbial abundance and composition influence litter decomposition response to environmental change. Ecology, 94, 714-725.

Allison, S. D., & Martiny, J. B. (2008). Resistance, resilience, and redundancy in microbial communities. Proceedings of the National Academy of Sciences, 105, 11512-11519.

Amor, D. R., Ratzke, C., & Gore, J. (2020). Transient invaders can induce shifts between alternative stable states of microbial communities. Science Advances, 6, eaay8676.

Anderegg, W. R., Schwalm, C., Biondi, F., Camarero, J. J., Koch, G., Litvak, M., ... & Wolf, A. (2015). Pervasive drought legacies in forest ecosystems and their implications for carbon cycle models. Science, 349, 528-532.

Berdugo, M., Delgado-Baquerizo, M., Soliveres, S., Hernández-Clemente, R., Zhao, Y., Gaitán, J. J., ... & Rillig, M. C. (2020). Global ecosystem thresholds driven by aridity. Science, 367, 787-790.

Berezovsky, I. N., & Shakhnovich, E. I. (2005). Physics and evolution of thermophilic adaptation. Proceedings of the National Academy of Sciences, 102, 12742-12747.

Birch, H. F. 1958. The effect of soil drying on humus decomposition and nitrogen availability. Plant and Soil, 10, 9–31.

Borsa, A. A., Agnew, D. C., & Cayan, D. R. (2014). Ongoing drought-induced uplift in the western United States. Science, 345, 1587-1590.

Conradi, T., Van Meerbeek, K., Ordonez, A., & Svenning, J. C. (2020). Biogeographic historical legacies in the net primary productivity of Northern Hemisphere forests. Ecology Letters, 23, 800-810.

Csonka, L. N. (1989). Physiological and genetic responses of bacteria to osmotic stress. Microbiological Reviews, 53, 121-147.

Cuddington, K. (2011). Legacy Effects: The Persistent Impact of Ecological Interactions. Biological Theory, 6, 203–210.

Evans, S.E., Wallenstein, M.D. (2012) Soil microbial community response to drying and rewetting stress: does historical precipitation regime matter? Biogeochemistry, 109**,** 101–116.

Evans, S. E., & Wallenstein, M. D. (2014). Climate change alters ecological strategies of soil bacteria. Ecology letters, 17, 155-164.

Falkowski, P. G., Fenchel, T., & Delong, E. F. (2008). The microbial engines that drive Earth's biogeochemical cycles. Science, 320, 1034-1039.

Ferenci, T. (2016). Trade-off mechanisms shaping the diversity of bacteria. Trends in Microbiology, 24, 209-223.

Fuchslueger, L., Bahn, M., Hasibeder, R., Kienzl, S., Fritz, K., Schmitt, M., ... & Richter, A. (2016). Drought history affects grassland plant and microbial carbon turnover during and after a subsequent drought event. Journal of Ecology, 104, 1453-1465.

Fukami, T. (2015). Historical contingency in community assembly: integrating niches, species pools, and priority effects. Annual Review of Ecology, Evolution, and Systematics, 46, 1-23.

Glassman, S. I., Weihe, C., Li, J., Albright, M. B., Looby, C. I., Martiny, A. C., ... & Martiny, J. B. (2018). Decomposition responses to climate depend on microbial community composition. Proceedings of the National Academy of Sciences, 115, 11994-11999.

Green, J.K., Seneviratne, S.I., Berg, A.M. *et al.* (2019). Large influence of soil moisture on long-term terrestrial carbon uptake. Nature, 565**,** 476–479.

Hawkes, C. V., & Keitt, T. H. (2015). Resilience vs. historical contingency in microbial responses to environmental change. Ecology letters, 18, 612-625.

Hawkes, C. V., Waring, B. G., Rocca, J. D., & Kivlin, S. N. (2017). Historical climate controls soil respiration responses to current soil moisture. Proceedings of the National Academy of Sciences, 114, 6322-6327.

Herzschuh, U. (2020). Legacy of the Last Glacial on the present-day distribution of deciduous versus evergreen boreal forests. Global Ecology and Biogeography, 29, 198-206

Hinojosa, M. B., Laudicina, V. A., Parra, A., Albert-Belda, E., & Moreno, J. M. (2019). Drought and its legacy modulate the post-fire recovery of soil functionality and microbial community structure in a Mediterranean shrubland. Global Change Biology, 25, 1409-1427.

Ives, A. R., & Carpenter, S. R. (2007). Stability and diversity of ecosystems. Science, 317, 58-62.

Kaisermann, A., de Vries, F. T., Griffiths, R. I., & Bardgett, R. D. (2017). Legacy effects of drought on plant–soil feedbacks and plant–plant interactions. New Phytologist, 215, 1413-1424.

Karhu, K., Auffret, M., Dungait, J. *et al.* (2014) Temperature sensitivity of soil respiration rates enhanced by microbial community response. Nature, 513, 81–84

Louca, S., Polz, M.F., Mazel, F. et al. (2018). Function and functional redundancy in microbial systems. Nature Ecology Evolution, 2, 936–943.

Malik, A.A., Martiny, J.B.H., Brodie, E.L. *et al.* (2020). Defining trait-based microbial strategies with consequences for soil carbon cycling under climate change. ISME J 14, 1–9.

Manzoni, S., Schimel, J. P., & Porporato, A. (2012). Responses of soil microbial communities to water stress: results from a meta-analysis. Ecology, 93, 930-938.

Martiny, J., Martiny, A., Weihe, C. et al. (2017). Microbial legacies alter decomposition in response to simulated global change. ISME J 11, 490–499.

McGill, B. J., Enquist, B. J., Weiher, E., & Westoby, M. (2006). Rebuilding community ecology from functional traits. Trends in Ecology & Evolution, 21, 178-185.

Meisner, A., Rousk, J., & Bååth, E. (2015). Prolonged drought changes the bacterial growth response to rewetting. Soil Biology and Biochemistry, 88, 314-322.

Moreno-Gámez, S., Kiviet, D. J., Vulin, C., Schlegel, S., Schlegel, K., van Doorn, G. S., & Ackermann, M. (2020). Wide lag time distributions break a trade-off between reproduction and survival in bacteria. Proceedings of the National Academy of Sciences, 117, 18729-18736.

Pellegrini, A., Ahlström, A., Hobbie, S. *et al.* (2018). Fire frequency drives decadal changes in soil carbon and nitrogen and ecosystem productivity. Nature, 553**,** 194–198.

Potts, M. (1994). Desiccation tolerance of prokaryotes. Microbiological Reviews, 58, 755-805.

Rousk, J., Smith, A. R., & Jones, D. L. (2013). Investigating the long-term legacy of drought and warming on the soil microbial community across five European shrubland ecosystems. Global Change Biology, 19, 3872-3884.

Scheffer, M., Carpenter, S., Foley, J. A., Folke, C., & Walker, B. (2001). Catastrophic shifts in ecosystems. Nature, 413, 591-596.

Schimel, J., Balser, T. C., & Wallenstein, M. (2007). Microbial stress-response physiology and its implications for ecosystem function. Ecology, 88, 1386-1394.

Staver, A. C., Archibald, S., & Levin, S. A. (2011). The global extent and determinants of savanna and forest as alternative biome states. Science, 334, 230-232.

583 Tikhonov, M., Kachru, S., & Fisher, D. S. (2020). A model for the interplay between plastic
584 tradeoffs and evolution in changing environments. Proceedings of the National Academy of
585 Sciences, 117, 8934-8940.
586
587 Tropini, C., Moss, E. L., Merrill, B. D., Ng, K. M., Higginbottom, S. K., Casavant, E. P., ... &
588 Bhatt, A. S. (2018). Transient osmotic perturbation causes long-term alteration to the gut
589 microbiota. Cell, 173, 1742-1754.
590
591 Wang, B., & Allison, S. D. (2019). Emergent properties of organic matter decomposition by soil
592 enzymes. Soil Biology and Biochemistry, 136, 107522.
593
594 Waring, B., Hawkes, C. V. (2018). Ecological mechanisms underlying soil bacterial responses to
595 rainfall along a steep natural precipitation gradient, FEMS Microbiology Ecology, 94, fiy001.
596
597 Vila, J. C., Jones, M. L., Patel, M., Bell, T., & Rosindell, J. (2019). Uncovering the rules of
598 microbial community invasions. Nature Ecology & Evolution, 3, 1162-1171.
599
600 Wieder, W. R., Allison, S. D., Davidson, E. A., Georgiou, K., Hararuk, O., He, Y., ... & Todd-
601 Brown, K., 2015. Explicitly representing soil microbial processes in Earth system models. Global
602 Biogeochemical Cycles, 29, 1782-1800.
603

Acknowledgements

All data and code underlying the analyses and illustrations in this manuscript (step-by-step analysis in Jupyter Notebook performed with Python) are accessible at: https://github.com/bioatmosphere/microbiome-drought-legacy. DEMENTpy code is available at: https://github.com/bioatmosphere/DEMENTpy. This research was funded by the NSF Ecosystem Studies Program (DEB-2016482) and the US Department of Energy Office of Science, BER, under award numbers DE-SC0016410 and DE-SC0020382.

Supporting Information

Drought Legacies Mediated by Trait Tradeoffs in Soil Microbiomes

Bin Wang [1], Steven D. Allison [1,2]

[1] Department of Ecology and Evolutionary Biology, University of California, Irvine, CA

[2] Department of Earth System Science, University of California, Irvine, CA

1 DEMENTpy

DEMENTpy is a trait-based modelling framework with spatially-explicit representation of individual populations in microbial communities. The model version reported here updates the physiological mechanisms (see **Supporting Fig. 1** for conceptual structure) and programming approach (see **Supporting Fig. 7** for programming structure) to the DEMENT model that was initially developed in 2012 (**Allison 2012**). The source code in Python is accessible at https://github.com/bioatmosphere/DEMENTpy. Processes simulated in DEMENTpy are described below.

1.1 Microbial community initialization

Using a trait-based approach, DEMENTpy initiates a microbial pool with a large number of hypothetical taxa by randomly drawing values from distributions of physiological traits (**Supporting Table 1**) and assigning them to different taxa. These hypothetical taxa in the microbial pool with differing combinations of trait values are randomly placed on the spatial grid to form a spatially structured microbial community. Illustrative animations are available at https://bioatmosphere.github.io/DEMENTpy/, and see **Wang and Allison (2019)** for an application of model spatial resolution for scaling up enzymatic heterogeneity. Trait distributions are all assumed to follow uniform distributions, except that for simplicity, some trait values are

assumed to be constant, and values of some traits are derived from established correlations with other traits. These distributions and assumptions are largely informed by field- and lab-based empirical studies (**Allison 2012; Allison and Goulden 2017**).

The key traits determining mass balance in drought simulations are constitutive and inducible rates of enzyme and osmolyte production. The richness of genes encoding different enzymes and osmolytes is determined randomly for each taxon during model initialization. Therefore, gene richness and production rate together determine the amounts of enzyme and osmolyte a cell can produce. The rate of inducible osmolyte production is then normalized to a value from 0 to 1, which is regarded as drought tolerance. This parameterization of drought tolerance is an update to the previous DEMENT version which instead directly introduced a drought tolerance parameter and imposed a penalty on carbon use efficiency accordingly (**Allison and Goulden 2017**). Linking osmolyte production directly to drought tolerance is intended to be more biologically realistic (**Schimel 2007**). Additionally, kinetic traits including Vmax and Km are assigned to explicitly parameterize a certain number of different enzymes and transporters in the model system.

1.2 Metabolic production of enzyme and osmolyte

Different individuals (hypothetical taxa) comprising the microbial community undergo demographic processes of growth, mortality, and reproduction while degrading substrates and assimilating monomers at rates dependent on temperature and water potential. From these underlying processes emerge dynamics and functioning at both the microbial cell level and the whole system level.

Substrate degradation rates are calculated based on the activities of enzymes with different kinetic properties. Every enzyme degrades at least one substrate, and every substrate is degraded

by at least one enzyme. Monomer uptake is calculated based on transporter abundance and kinetic traits which are specific to each taxon. The governing equation for both substrate degradation and monomer uptake follows the Michaelis-Menten equation, which is constrained by temperature (accounting for temperature impacts on enzymatic kinetics) and water potential (accounting for moisture constraints on enzymatic kinetics and diffusion; **Allison and Goulden 2017**):

$$V = \frac{V_{max} f(T)[S][E]}{K_m + [S]} f(\psi)$$

$$f(T) = e^{\left(-\frac{\boldsymbol{\varepsilon}}{R}\left(\frac{1}{T} - \frac{1}{T_{ref}}\right)\right)}$$

$$f(\psi) = e^{k\psi}$$

where *E* and *S* are matrices containing enzyme and substrate concentrations, respectively, *Vmax* represents the enzyme catalytic constant, K_m denotes the concentration of *S* at which *V* is one half V_{max}, $\boldsymbol{\varepsilon}$ is enzymatic activation energy, *R* is universal gas constant, and *k* is a coefficient controlling water potential sensitivity that differs between degradation and uptake.

Cellular metabolism balances carbon upon uptake from degraded substrates and carbon loss through constitutive and inducible metabolite production (**Supporting Fig. 3**). After growth respiration (constrained by a constant), assimilated carbon is directed to enzyme and osmolyte production along with their associated maintenance respiration rates, all of which are treated simultaneously in the model without prescribing an order. The carbon remaining after these processes accumulates toward biomass. We assume the constitutive osmolyte production rate (*Osmo_Con*) varies across taxa independent of water potential, accounting for microbial allocation to maintain water potential balance across the cell wall (**Csonka 1989; Potts 1994**). In contrast, taxon-specific inducible production of osmolytes (O_{ind}) depends on water potential as follows:

$$O_{ind}(i) = \begin{cases} O_{ind}(i), & \psi \geq \psi_{th} \\ O_{ind}(i)\ (1\ -\ \alpha\psi), & \psi < \psi_{th} \end{cases}$$

where O_{ind}, is the i_{th} taxon's inducible osmolyte production rate, ψ is the daily water potential, α is a coefficient determining water potential sensitivity, and ψ_{th} is a system water potential constant, below which inducible osmolyte production is activated. Osmolyte stoichiometry is assumed to be constant at C/N = 3, which governs consumption of N in intracellular metabolism. This ratio is based on an average of the three most common osmotic compounds in bacteria (**Csonka 1989; Potts 1994**): proline ($C_5H_9NO_2$), glycine betaine ($C_5H_{11}NO_2$), and glutamine ($C_5H_{10}N_2O_3$).

Mortality of microbial cells is simulated both deterministically by accounting for mass balance relative to a threshold, and stochastically based on a death probability constrained by drought tolerance and water potential. Here the taxon-specific mortality probability (*Mort*) is calculated as:

$$Mort_i = Death\_basal_i[1 - Death\_rate_i(1 - Tol_i)(\psi - \psi_{th})\ ]$$

where *Death_basal* is the i_{th} taxon's basal mortality probability, *Death_rate* is a death probability coefficient controlling water potential sensitivity, *Tol* is the i_{th} taxon's drought tolerance, and ψ_{th} is a system water potential constant. Microbial cells that fall below the biomass threshold or that die randomly are removed from the microbial community and added into the substrate pools as dead microbes. Microbial reproduction is calculated by splitting microbes into two equal halves, followed by local dispersal to surrounding grid boxes on the spatial grid (**Allison 2012**).

2. Calculation of community-level traits

Community-level enzyme investment (E_{com}) and drought tolerance (D_{com}) weighted by biomass are calculated as:

$$E_{com} = \sum_{i}^{n} EiMi$$

$$D_{com} = \sum_{i}^{n} DiMi$$

respectively, where *Ei* and *Di* refer to the i_{th} taxon's enzyme production rate and drought tolerance, respectively, and *Mi* is the relative biomass of the i_{th} taxon in the community.

References

Allison, S. D. (2012). A trait-based approach for modelling microbial litter decomposition. Ecology letters, 15, 1058-1070.

Allison, S. D., & Goulden, M. L. (2017). Consequences of drought tolerance traits for microbial decomposition in the DEMENT model. Soil Biology and Biochemistry, 107, 104-113.

Bugmann, H., Fischlin, A., & Kienast, F. (1996). Model convergence and state variable update in forest gap models. Ecological Modelling, 89, 197-208.

Csonka, L. N. (1989). Physiological and genetic responses of bacteria to osmotic stress. Microbiological Reviews, 53, 121-147.

Potts, M. (1994). Desiccation tolerance of prokaryotes. Microbiological Reviews, 58, 755-805.

Schimel, J., Balser, T. C., & Wallenstein, M. (2007). Microbial stress-response physiology and its implications for ecosystem function. Ecology, 88, 1386-1394.

Wang, B., & Allison, S. D. (2019). Emergent properties of organic matter decomposition by soil enzymes. Soil Biology and Biochemistry, 136, 107522.

Supporting Table 1 Microbial and enzyme parameters and their values

Parameter	Value	Unit	Note
max_size_b	2	mg cm-3	C quota threshold for bacterial cell division
Cfrac_b	0.825	mg mg-1	Bacterial C fraction
Nfrac_b	0.16	mg mg-1	Bacterial N fraction
Pfrac_b	0.015	mg mg-1	Bacterial P fraction
Crange	0.09	mg mg-1	Tolerance on C fraction
Nrange	0.04	mg mg-1	Tolerance on N fraction
Prange	0.005	mg mg-1	Tolerance on P fraction
C_min	0.086	mg cm-3	threshold C concentration for cell death
N_min	0.012	mg cm-3	threshold P concentration for cell death
P_min	0.002	mg cm-3	threshold C concentration for cell death
Uptake_C_cost_min	0.01	transporter mg-1 biomass C	Minimun per enzyme C cost as a fraction of uptake
Uptake_C_cost_max	0.1	transporter mg-1 biomass C	Maximum per enzyme C cost as a fraction of uptake
Uptake_Maint_cost	0.01	mg C transporter-1 day-1	Respiration cost of uptake transporters
Enz_per_taxon_min	0		Minimum number of enzymes a taxon can produce
Enz_per_taxon_max	40		Maximum number of enzymes a taxon can produce
Enz_Prod_min	0.00001	mg C mg-1 day-1	Minimum per enzyme production cost as a fraction of C uptake rate
Enz_Prod_max	0.0001	mg C mg-1 day-1	Maximum per enzyme producton cost as a fraction of C uptakte rate
Constit_Prod_min	0.00001	mg C mg-1 day-1	Minimum per enzyme production cost as a fraction of biomass C
Constit_Prod_max	0.0001	mg C mg-1 day-1	Maximum per enzyme production cost as a fraction of biomass C
Osmo_per_taxon_min	1		Minimum number of osmolyte a taxon can produce
Osmo_per_taxon_max	1		Maximum number of osmolyte a taxon can produce
Osmo_Consti_Prod_min	0.0000001	mg C mg-1 day-1	Minimum per osmolyte production cost as a fraction of biomass C
Osmo_Consti_Prod_max	0.000001	mg C mg-1 day-1	Maximum per osmolyte production cost as a fraction of biomass C
Osmo_Induci_Prod_min	0.01	mg C mg-1 day-1	Minimum per osmolyte production cost as a fraction of C uptake rate
Osmo_Induci_Prod_max	0.1	mg C mg-1 day-1	Maximum per osmolyte production cost as a fraction of C uptake rate
CUE_ref	0.5	mg mg-1	Growth efficiency at the reference temperature
CUE_temp	-0.005	mg mg-1	Growth efficiency change with enzyme investment
death_rate_bac	0.001		Bacterial death rate
basal_bac	10		Bacterial basal death probability
wp_th	-2.00	MPa	Water potential threshold at which osmolyte is induced
alpha	0.01	mg C mg-1 day-1	Osmolyte production change with water potential
Vmax0_min	5	mg substrate mg-1 enzyme day-1	Minimum Vmax for enzyme
Vmax0_max	50	mg substrate mg-1 enzyme day-1	Maximum Vmax for enzyme

Uptake_Vmax0_min	1	mg substrate mg-1 substrate day-1	Minimum uptake Vmax
Uptake_Vmax0_max	10	mg substrate mg-1 substrate day-1	Maximum uptake Vmax
Uptake_Ea_min	35	kj mol-1	Minimum activation energy for uptake
Uptake_Ea_max	35	kj mol-1	Maximum activation energy for uptake
Km_min	0.01	mg cm-3	Minimum Km
Uptake_Km_min	0.001	mg cm-3	Minimum uptake Km
Vmax_Km	1	mg enzyme day cm-3	Slope for Km-Vmax relationship
Vmax_Km_int	0	mg cm-3	Intercept for Km-Vmax relationship
Uptake_Vmax_Km	0.2	mg biomass day cm-3	Slope for uptake Km-Vmax relationship
Uptake_Vmax_Km_int	0	mg cm-3	Intercept for uptake Km-Vmax relationship
Specif_factor	1		Enzyme efficiency-specificity

Supporting Table 2 Substrate concentrations initialized in DEMENT simulations (mg cm^{-3}).

Substrate	C	N	P
DeadMic	0	0	0
DeadEnz	0	0	0
Cellulose	146.89	0	0
Hemicellulose	85.855	0	0
Starch	12.21	0	0
Chitin	4.9952	0.83254	0
Lignin	48.51	0.40425	0
Protein1	10.6	2.09704	0
Protein2	10.6	2.09704	0
Protein3	10.6	2.09704	0
OrgP1	12.48	0	0.478469
OrgP2	1.8182	0.79745	0.478469

121

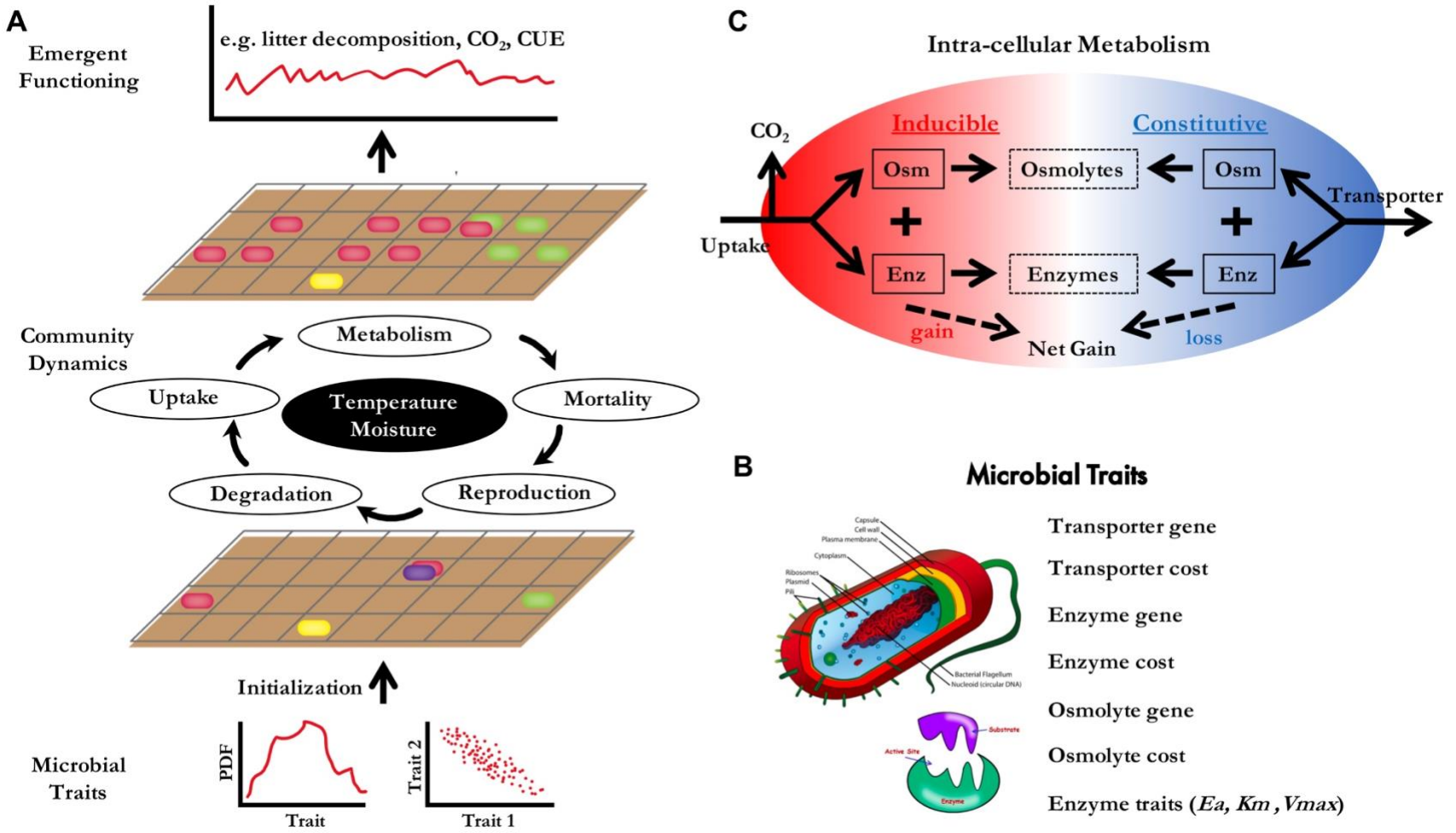

122

123 **Supporting Fig. 1 DEMENTpy conceptual structure (A), microbial traits (B), and intra-cellular metabolism (C).**

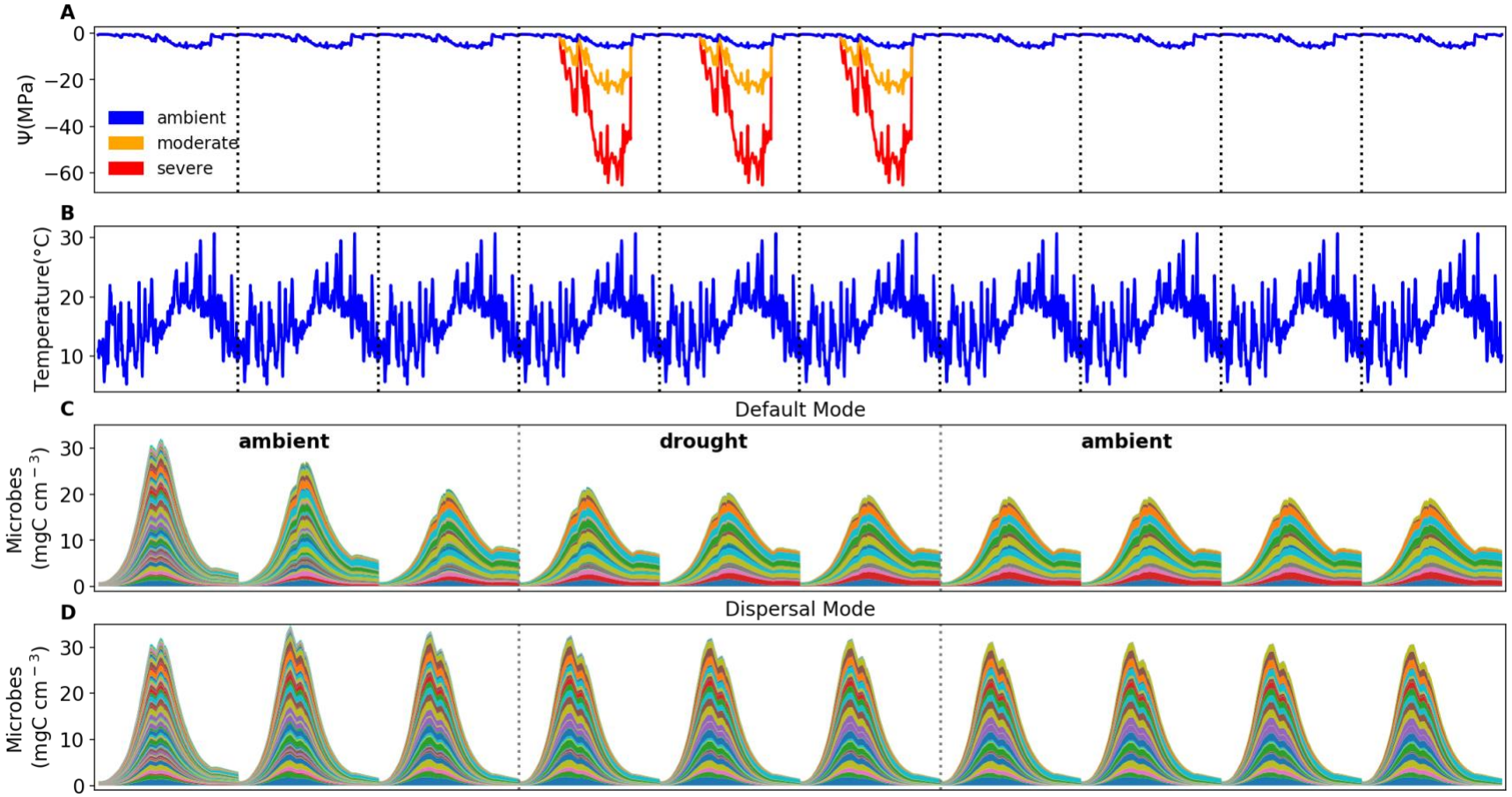

Supporting Fig. 2 Environmental forcing and microbial community dynamics. (**A**) Ambient daily water potential for 2011, with the orange and red lines denoting the moderate and severe drought scenarios, respectively. Drought forcing was obtained by multiplying the ambient water potential across the dry season (from April through September) by 4 and 10, respectively. (**B**) The corresponding daily temperature in 2011. (**C, D**) Microbial community dynamics of the default vs. dispersal mode over 10 years under the ambient

scenario. The simulation comprises three phases as separated by the dashed grey lines: a spin-up phase of three years to realize a relatively stable community; a disturbance phase imposing different drought scenarios for three years; and a final recovery phase after drought disturbance for four years. Colored bands represent biomasses of hypothetical taxa.

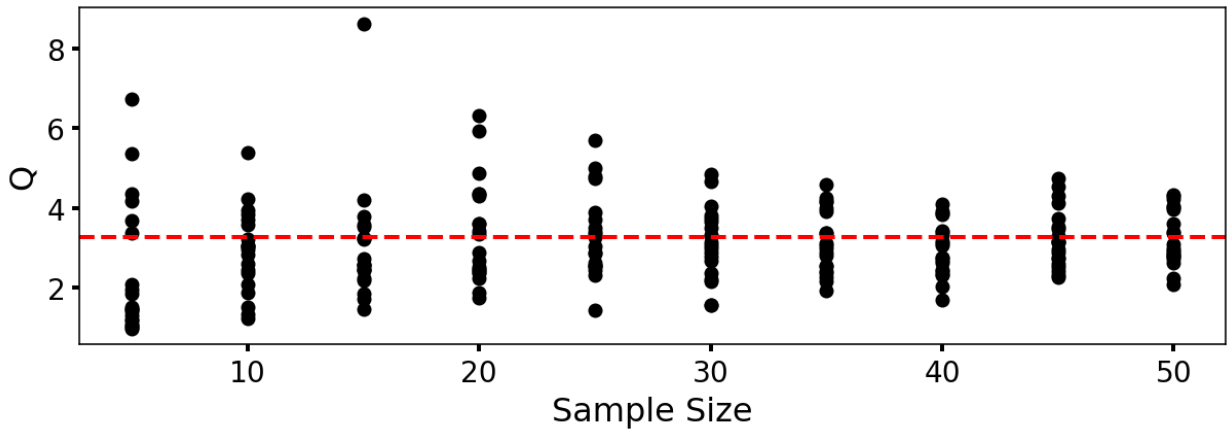

Supporting Fig. 3 DEMENTpy (v1.0) stochasticity convergence analysis. Q (quotient) is calculated as (90% percentile -10% percentile)/median substrate degradation following Bugmann et al. (1996). Each sample size has 20 replicates that were randomly drawn from a sample pool of 112 runs. This analysis illustrates that a sample size (i.e., ensemble of simulations) of 40 displays relatively stable, convergent variation and that balances the tradeoff between precision and. consumption of computing resources.

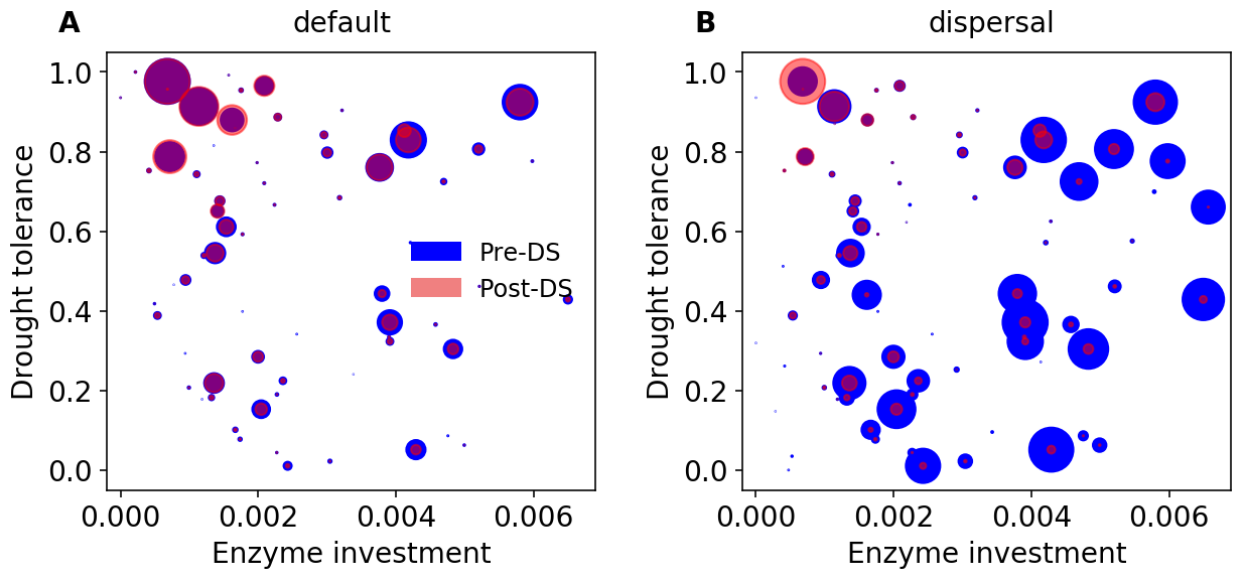

Supporting Fig. 4 Taxonomic changes in traits across the dry season. (A) Taxon-specific traits of drought tolerance and enzyme investment of a microbial community without dispersal before (blue) and after the dry season (red) under the ambient scenario. (**B**) The same for a microbial community with dispersal. Each point corresponds to a different taxon, and the size is proportional to its biomass.

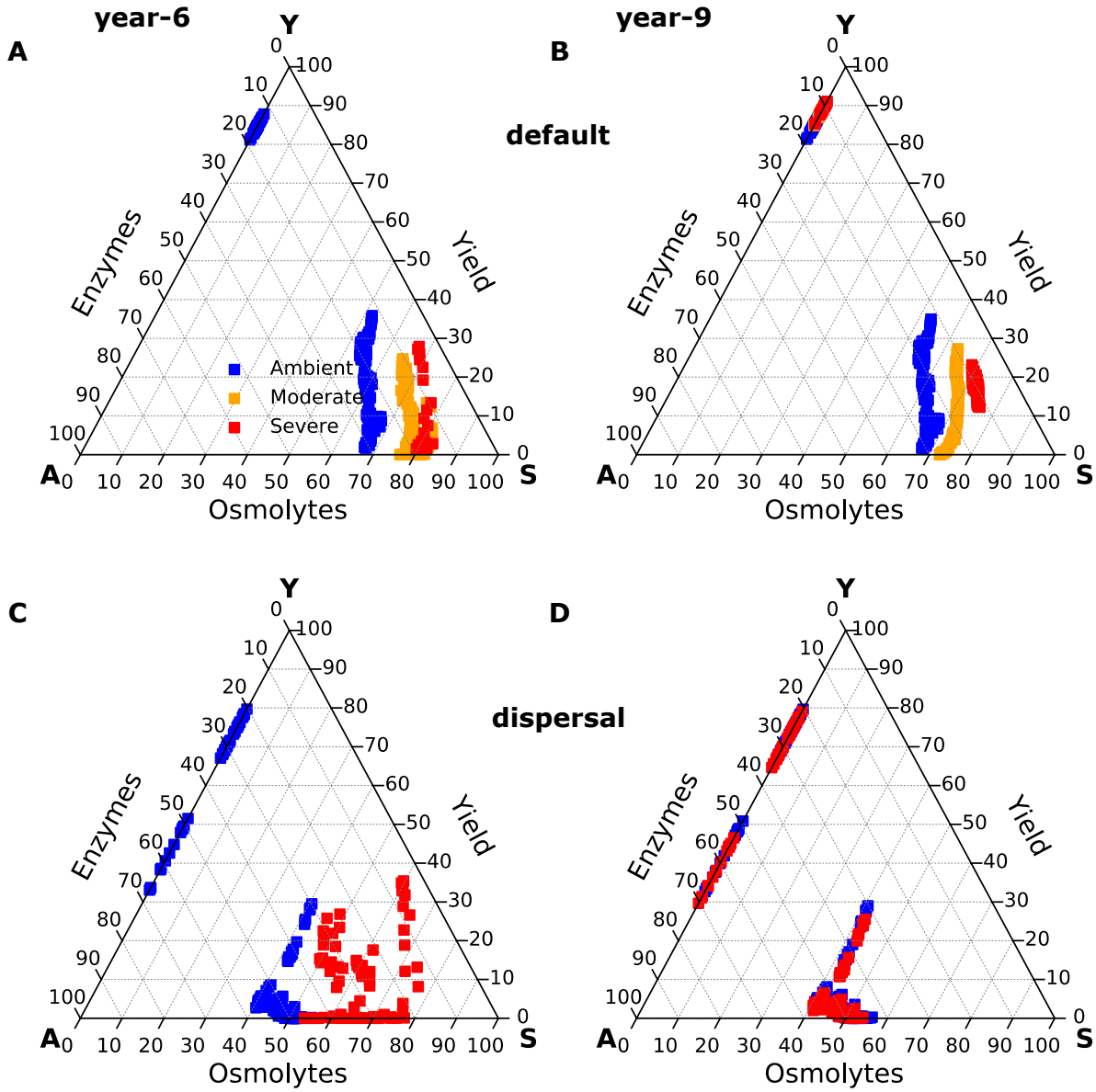

145

146 **Supporting Fig. 5 Ternary plots of community-level allocation of assimilated carbon among**
147 **enzymes, osmolytes, and yield over time under different drought scenarios. (A, B)** Enzyme-
148 Osmolyte-Yield tradeoff of communities during year 6 (3rd year under drought) and year 9 (3rd
149 year after drought), respectively, of the default mode (without dispersal). **(C, D)** The same for the
150 dispersal mode. The Y (Yield), A (Acquisition), and S (Stress tolerance) labels at the vertices

correspond to yield, enzymes, and osmolytes, respectively. Points with negative net biomass gain were omitted.

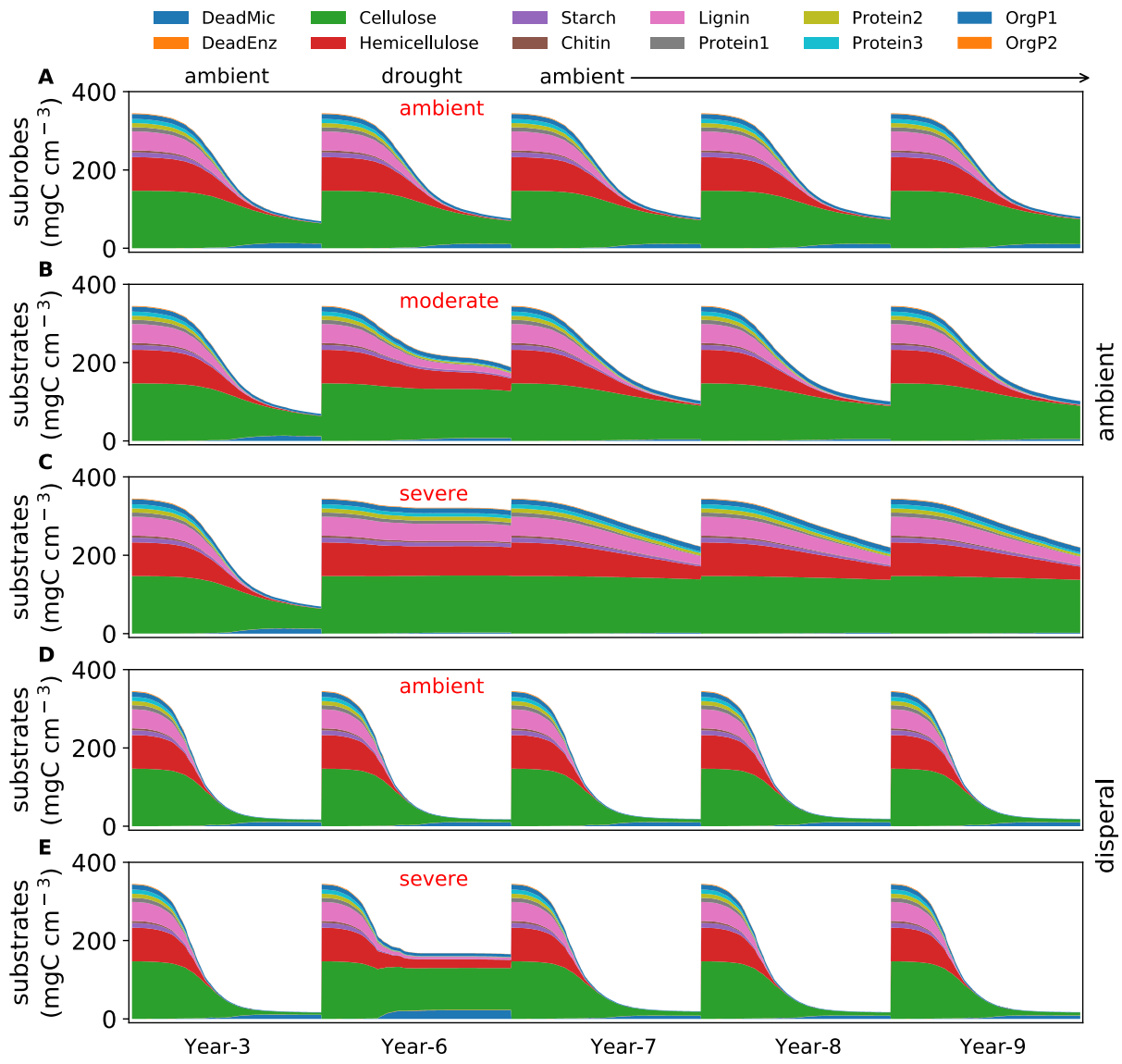

154

155 **Supporting Fig. 6 Substrate-specific dynamics under differing drought scenarios. (A, B, C)**

156 Dynamics under ambient, moderate, and severe drought scenarios in default mode for year 3 and

157 year 6 (the 3rd year under drought disturbance) through year 9. (**D, E**) The same for the dispersal

158 mode but with only ambient and severe scenarios. Each color band represents one type of 12

159 different substrates.

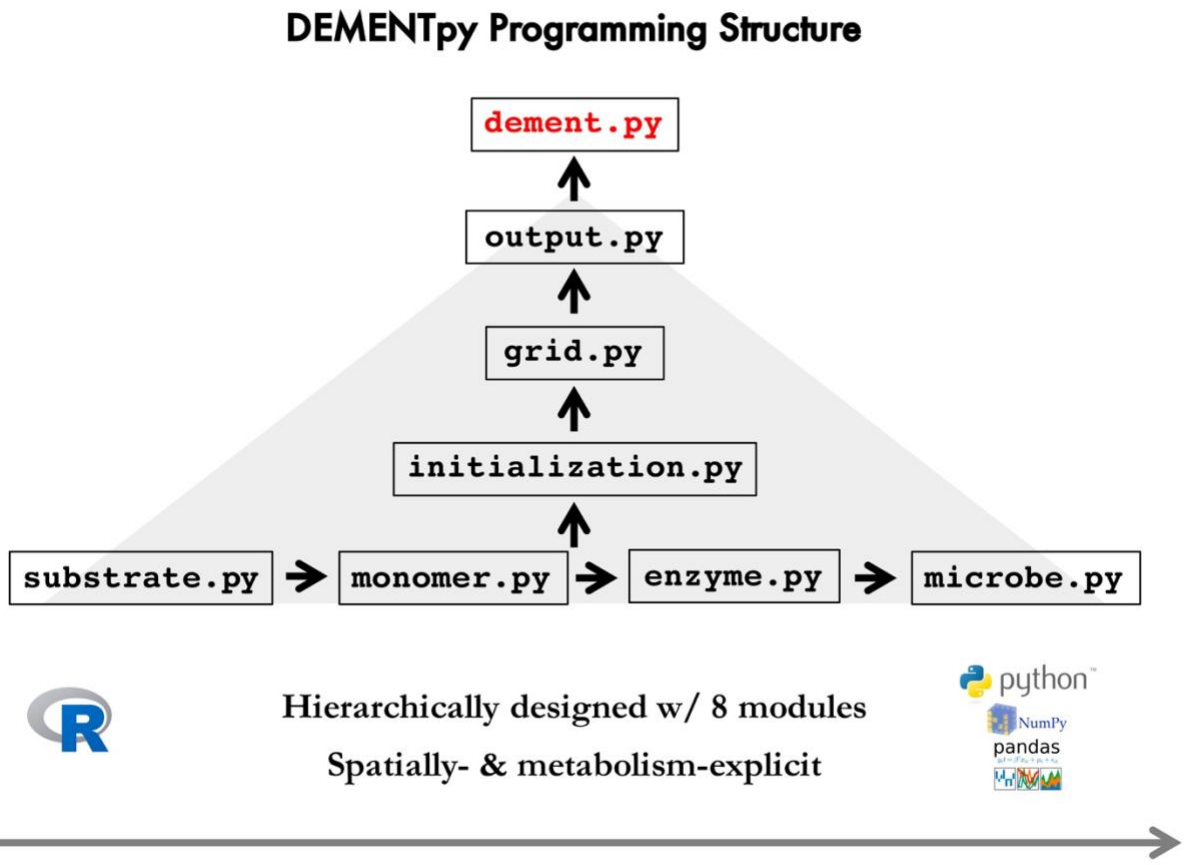

Supporting Fig. 7 DEMENTpy programming structure. DEMENTpy emerges from hierarchically restructuring and mechanistically updating DEMENT, which was programmed in R.